JTTEE5 17:105–114
DOI: 10.1007/s11666-007-9143-3
1059-9630/$19.00 © ASM International

Suspension Plasma Spraying of YPSZ Coatings: Suspension Atomization and Injection

Régine Rampon, Claudine Filiatre, and Ghislaine Bertrand

(Submitted March 30, 2007; in revised form July 13, 2007)

Among processes evaluated to produce some parts of or the whole solid-oxide fuel cell, Suspension Plasma Spraying (SPS) is of prime interest. Aqueous suspensions of yttria partially stabilized zirconia atomized into a spray by an internal-mixing co-axial twin-fluid atomizer were injected into a DC plasma jet. The dispersion and stability of the suspensions were enhanced by adjusting the amount of dispersant (ammonium salt of polyacrylic acid, PAA). A polyvinyl alcohol (PVA) was further added to the suspension to tailor its viscosity. The PVA also improved the dispersion and stability of the suspensions. The atomization of optimized formulations is described implementing Weber and Ohnesorge dimensionless numbers as well as gas-to-liquid mass ratio (ALR) value. Drop size distributions changed from monomodal distributions at low *We* to multimodal distributions when *We* number increases. The viscosity of the suspensions has a clear influence on the drop size distribution and suspension spray pattern. The secondary fragmentation of the drops due to the plasma jet was evidenced and the final size of the sheared drops was shown to depend on the characteristics of the suspension. Rather dense zirconia coatings have been prepared, which is a promising way to produce electrolyte.

Keywords droplets, SOFC, suspension injection, suspension plasma spraying, yttria-stabilized zirconia

1. Introduction

Since the late 1990s, an increasing number of works have been devoted to the realization of the whole solid-oxide fuel cell by plasma spraying (Ref 1-6). Indeed, the most important advantage of this technology versus conventional ones, such as screen printing, tape casting, etc, relies in the ability to manufacture the entire IT-SOFC with the same process. Plasma spraying processes show great potential for bringing down the production costs. This technology also permits to easily modify the design and compositions of the electrodes as well as the electrolyte. The latter has been the focus of numerous research activities that aim at producing dense and thin (10-30 μm) yttria partially stabilized zirconia (Y-PSZ) coatings. The reduction of the electrolyte oxygen-ion conducting layer thickness tends to decrease the working temperature of SOFC, increasing in turn their lifetime and hence to reduce the internal electrical resistance of the cell (ohmic losses) (Ref 7-9).

Régine Rampon and **Ghislaine Bertrand**, Laboratoire d'Etudes et de Recherches sur les Matériaux, les Procédés et les Surfaces (LERMPS), Université de Technologie de Belfort Montbéliard (UTBM), Site de Sévenans, 90010 Belfort Cedex, France; and **Claudine Filiatre**, Institut UTINAM – UMR CNRS 6213, UFR des Sciences et Techniques, 16 route de Gray, Bât. C, 25030 Besancon, France. Contact e-mail: ghislaine.bertrand@utbm.fr.

Y-PSZ coatings were plasma sprayed under controlled atmosphere at reduced pressure (VPS) to increase the plasma jet velocity using plasma torches with De Laval nozzles, resulting in enhanced impact velocity of the spray particles. The improved momentum of the melted particles (impact velocity of about 650 m/s) favors thinner and denser layers (Ref 10-15). Around 20 μm thick Y-PSZ and ScSZ (Scandia-Stabilized Zirconia) coatings were achieved at the German Aerospace Center (DLR for Deutsche Zentrum für Luft- und Raumfahrt) with deposition yield of 7 μm/pass (Ref 11-13). The porosity, evaluated by image analysis, was found below 2.5%. However, the authors have shown that the leak rate decreases when increasing the electrolyte thickness and the optimum selected to limit the ohmic resistance was in the range of 40-50 μm. This has been further improved by annealing the samples during 50 h at 1100 °C. Even in such conditions the ionic conductivity of the Y-PSZ and ScSZ electrolytes was still lower compared to the sintered ones.

Atmospheric plasma Spraying (APS) process, often combined to additional heat treatments, was also investigated as a promising technology to produce electrolyte for SOFCs. As-sprayed ceramic coatings, resulting from lamella stacking, contain interlamellar and intralamellar connected pores which form an interconnected network which impedes the ionic conductivity of the electrolyte. The sintering stage is under those conditions required to densify the as-sprayed electrolyte. Conventional and nonconventional (such as spark plasma sintering for example) sintering processes have been investigated (Ref 16-18). The possibility to add a sintering agent, such as MnO_2 to YSZ, demonstrated to be appropriate for reducing the sintering temperature (from

1550 to 1400 °C for 5 wt.% of MnO_2) to obtain gas tightness. Implementing a rapid consolidation technique, such as spark plasma sintering, significantly improves the ionic conductivity of electrolytes (twofold as compared to as-sprayed coatings) due to changes in the structure from lamellar to granular resulting in porosity decrease. In parallel, some authors implementing a three-cathode Triplex II APS torch have demonstrated that it is possible by optimizing the powder characteristics and the particle temperature and velocity to drastically reduce the volume density and size of connected cracks developing in 50 μm thick Y-PSZ coatings and thus the leakage rate (Ref 19). Such optimized coating structures should allow to avoid post heat treatment.

Alternate processes rely on the solution precursor plasma spraying (SPPS) and the suspension plasma spraying (SPS) which consist in injecting a solution of the elements to be deposited or a suspension of sub-micrometer particles dispersed in a liquid, respectively, into DC or RF plasma torches (Ref 20-30). These processes, which appeared almost a decade ago for the very first trials and are nowadays more systematically studied, allow producing finely structured coatings. Recent works have been published on zirconia-based SPS, which demonstrate the potential of this process regarding the elaboration of the electrolyte layer. Considering DC plasma spraying, the suspension is commonly injected radially into the plasma jet externally to the torch, either as a straight jet or as an atomized one. It has been shown that the coating density is improved by enhancing the penetration of the liquid feedstock within the plasma jet, either by optimizing the injection system (from a nebulized to a liquid or droplet jet) or by adjusting both the plasma jet and the liquid characteristics (suspension momentum density, injection angle, plasma gas mixture and mass rate, etc) (Ref 31-36). A mechanical injection (single precision hole injector with pressurized tanks or continuous ink jet printer) is often preferred because it provides a stream of drops of homogenized size and velocity which should then be more homogeneously treated in the plasma flow. Considering SPS conditions (i.e., radial injection of the suspension), it was shown that the liquid velocity as well as location and injection angle are critical to ensure effective heat and momentum transfers to the droplets which seem to lead to dense ceramic coating (Ref 31, 33, 37-39). But very few studies have been devoted to assess the effects of the suspension characteristics on the atomization mechanisms or on drop formation and thus on their behavior in the plasma.

In the present study, the suspensions were atomized into a spray by a bi-fluid atomizer that generates droplets. These droplets were injected radially into a DC plasma jet where they were accelerated and heated. This article aims at studying the importance of the suspension characteristics on the successive steps leading to the coating formation.

The experimental set-ups are first described. The suspension composition and its physical and chemical properties are highlighted. Then the characterization of the suspension atomization is discussed and the evolutions encountered by the drops and particles in the plasma are evaluated. Finally, the microstructures of the coatings produced by SPS are presented and discussed.

2. Experimental Facilities

2.1 Plasma Spraying Set-Up

The spraying system consists of an atmospheric F4-VB plasma torch (Sultzer-Metco AG, Wohlen, Switzerland) mounted on an ABB robot to ensure an accurate control of the speed and motion of the torch in front of the substrate. The internal diameter of the anode nozzle is 6 mm. Moreover, the plasma torch voltage (V) and arc current intensity (I) as well as thermal losses (Q) at the electrodes are measured. The effective torch power ($P = VI - Q$) and the specific enthalpy ($h = P/m$ where m is the total plasma gas mass flow rate) of the plasma jet are deduced from the previous parameters. The operating conditions are reported in Table 1.

An external injection system developed at the laboratory was used to ensure the atomization before radial injection of the droplets into the Ar-H_2 plasma under atmospheric conditions. The mechanically stirred suspension is delivered by a peristaltic pump in the atomizer-injector nozzle which is located onto a ring fixed on the torch nozzle. The suspension droplets are counter-flow injected in the plasma with an angle of 15° and the feed rate is measured for each operating condition (pump speed and suspension formulation). The atomization of the suspension is achieved by a two fluid nozzle in which the energy for atomization is provided by the rapid expansion of a gas (Ar) which is mixed with the suspension within the body of the nozzle (internally mixing).

2.2 Suspension and Droplets Characterization

Y-PSZ powder (ZrO_2-8 wt.%Y_2O_3) with a specific surface area of 6.7 m^2/g (N_2 BET method) and d_{50} of 0.6 μm (d_{10} of 0.3 μm and d_{90} of 0.9 μm) supplied by Saint-Gobain Ceramic Materials (Le Pontet, France) was used to achieve the aqueous suspensions. The solid loading of the suspension was fixed at 20 wt.% according to an already published work (Ref 40) in which this value was found to be a good compromise between deposition efficiency and required plasma output.

The stability and dispersion of the 20 wt.% Y-PSZ-loaded suspensions were assessed by performing sedimentation tests and particle size distribution measurements. To study the sedimentation rates and the settling volumes for long times, the suspension which is poured into a tube is crossed by a near-IR light (880 nm) and the intensities of the backscattered and transmitted

Table 1 Plasma operating conditions for F4-VB type plasma torch

Arc current, A	600
Effective power, kW	19.8
Specific enthalpy, MJ/kg	23.6
Plasma gas mixture	Ar-H_2 (30-8 slpm)
Internal nozzle diameter, mm	6
Stand-off distance, mm	40

lights are measured versus time using a TurbiScan Lab® Expert apparatus (Formulaction, l'Union, France). The particle size distribution was checked by laser light diffusion implementing a Mastersizer2000 (Malvern Instruments, Orsay, France).

The rheological measurements of the slurries were conducted using a controlled stress rheometer Carrimed CSL50 with cone-plate geometry from Rheo (Clermont Ferrand, France). Newly formulated samples were agitated and then measured immediately. Flow curves were automatically recorded according to the following input: the shear stress increased continuously from 0 to 3.5 or 10 Pa over a period of 1 min and then reversed from 3.5 or 10 to 0 Pa in 1 min. The shear stress maximum value was adjusted according to the suspension behavior. All the experiments were performed at a temperature of 20 °C. The surface tension characteristics were also determined using a tensiometer K12 from Krüss (Hamburg, Germany) based on the Wilhelmy's plate method (a roughened platinum plate is raised until the contact between the surface and the plate is registered and the surface tension is then calculated from the wrenching force).

The droplet size distributions, before entering the plasma, have been measured at 6 mm from the atomizing nozzle exit (this value corresponds to the injector to torch axis distance) using the Spraytech system (Malvern Instruments, Orsay, France), which principle is based on laser light scattering (Mie diffraction theory). Various parameters were evaluated; such as the argon and suspension flow rates as well as the suspension formulation.

3. Results and Discussion

In the present study, all the experiments were achieved implementing aqueous suspensions of Y-PSZ particles. In contrast to organic solvents like ethanol, water has higher boiling point (373 K) and heat of vaporization (2256 kJ/kg).

3.1 Effects of the Formulation on the Suspension Behavior

In a previous study (Ref 41), the isoelectric point (IEP) of the Y-PSZ particles was established at pH 5.8 and an anionic dispersant—ammonium salt of polyacrylic acid ($PAANH_4$) with an average molecular weight of 7000-8000 g/mol (Coatex S.A., Lyon, France)—was found appropriate to achieve dispersed suspensions. At a neutral pH, which was chosen for the present study, the particles were slightly negative and the PAA adsorption saturation limit was determined at 0.3 mg/m^2 (based on PAA adsorption isotherms). As the PAA is negatively charged at that pH value, a low amount of dispersant is required to fully cover the particles (about 0.17 wt%— percentage related to the weight of solid particles) and to achieve an electrosteric dispersion of the suspension. The addition of 0.17 wt.% of dispersant leads to an increase in the stability of the suspension as reported in Fig. 1 and of the dispersion as shown in Fig. 2(a) and (b). Indeed, without dispersant, flocculation occurs very quickly after stirring is stopped giving agglomerates of a few hundreds of micrometers in diameter, which form a sediment in about 50 min. In contrast, the addition of dispersant maintains the particle size around 2 μm in diameter limiting the sedimentation. It can also be noticed from Fig. 2(a) and (b) that the size of the particles in the suspensions with dispersant are larger than the size of the initial particles which have a size distribution centered at 0.6 μm.

In order to change the viscosity of the previously formulated suspension, a polyvinyl alcohol (PVA from Rhodia, Lyon, France) was added. Increasing the amount of PVA up to 20 wt.% (related to the weight of solid particles) is very efficient to enhance the stability of the suspension as shown in Fig 3. At the same time the dispersion of the particles is also improved by the addition of PVA (Fig. 2c) leading to a fully dispersed suspension when 0.17 wt.% PAA and 12 wt.% PVA are mixed (particle size distribution is now centered around 0.6 μm). The combined effect of both organic additives to enhance

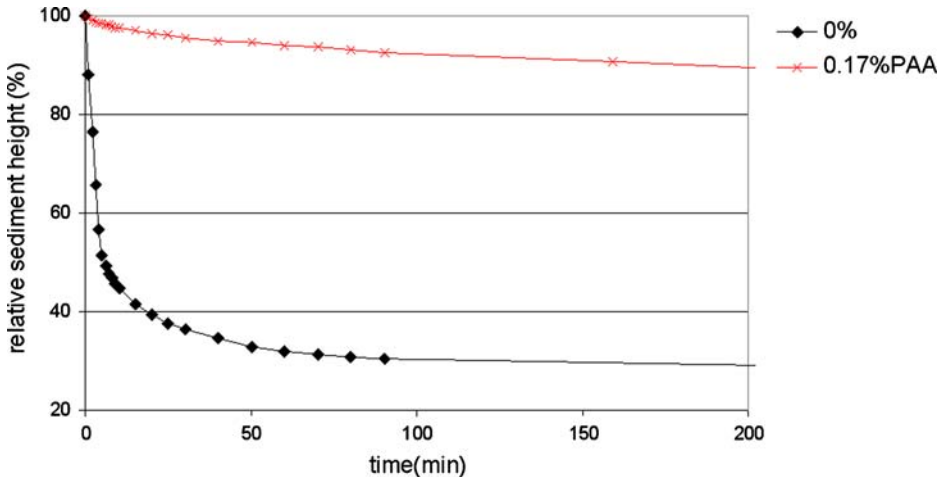

Fig. 1 Evolution of the relative sediment height vs. time of 20 wt.% Y-PSZ aqueous suspensions without and with 0.17 wt.% PAA

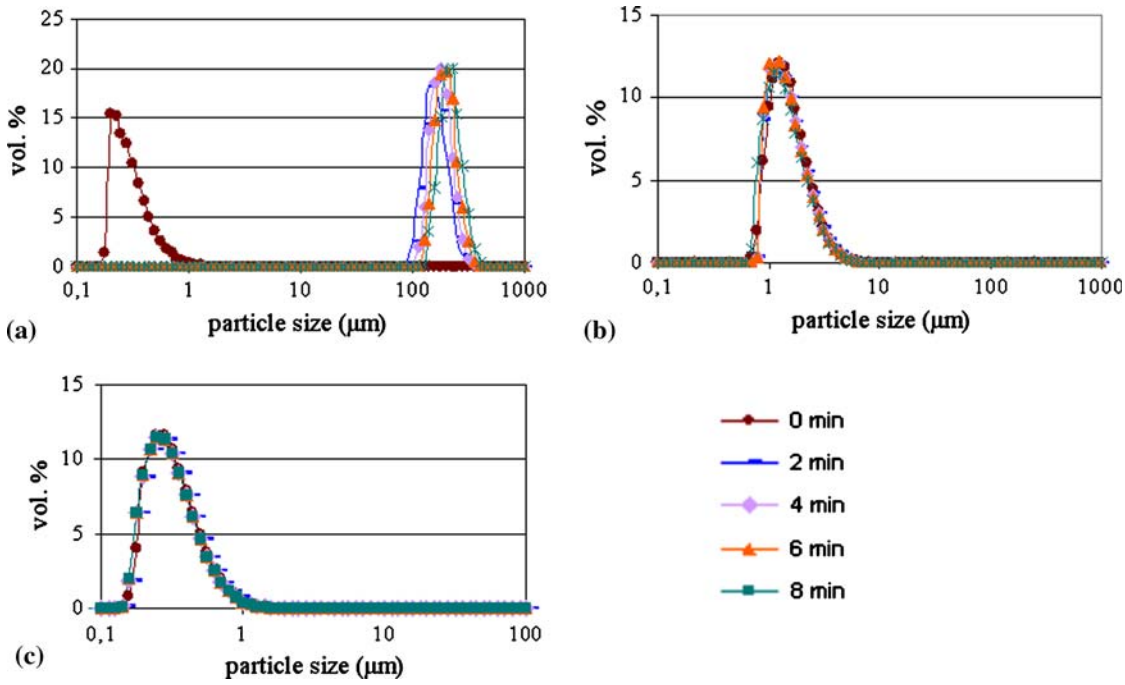

Fig. 2 Evolution of the particles size distribution vs. time for three 20 wt.% Y-PSZ aqueous suspensions (a) without, 9b) with 0.17 wt.% PAA, and (c) with 0.17 wt.% PAA and 12 wt.% PVA

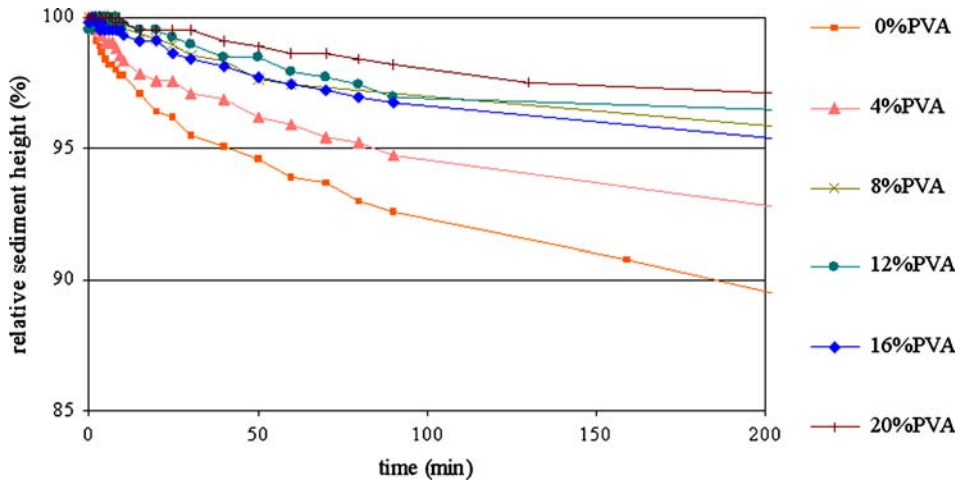

Fig. 3 Evolution of the relative sediment height with vs. time of 20 wt.% Y-PSZ aqueous suspensions loaded with 0.17 wt.% PAA and various amounts of PVA ranging from 0 to 20 wt.%

the stability and dispersion of the Y-PSZ aqueous suspension is clearly evidenced. It could be assumed that the hydroxyl groups of the PVA are interacting with the negatively charged carboxylic groups of the PAA avoiding the particles interactions and increasing the steric shielding effect. The rheological flow curves for Y-PSZ suspensions as a function of PVA concentration are shown in Fig. 4. As can be noticed, the Y-PSZ suspensions (with 0.17 wt.% PAA) exhibit a shear thinning and thixotropic behavior whatever the amount of PVA. However, the hysteresis decreases as the amount of PVA increases. As a consequence, viscosity decreases with shear rate ranging from 4 mPa.s without PVA to 6 mPa.s with 8 wt.% PVA and to 14 mPa.s with 16 wt.% PVA (Fig. 5). The addition of PVA increases the viscosity of the Y-PSZ suspensions probably because at such high concentration levels PVA remains appreciably present in the solution. In contrast, the surface tension is constant around 38 mN/m whatever the formulation of the suspension, a much lower value than the one of water (about 73 mN/m at 293 K).

Finally, three formulations have been selected with 20 wt.% of YPSZ, 0.17 wt.% of PAA, and 0, 8, and

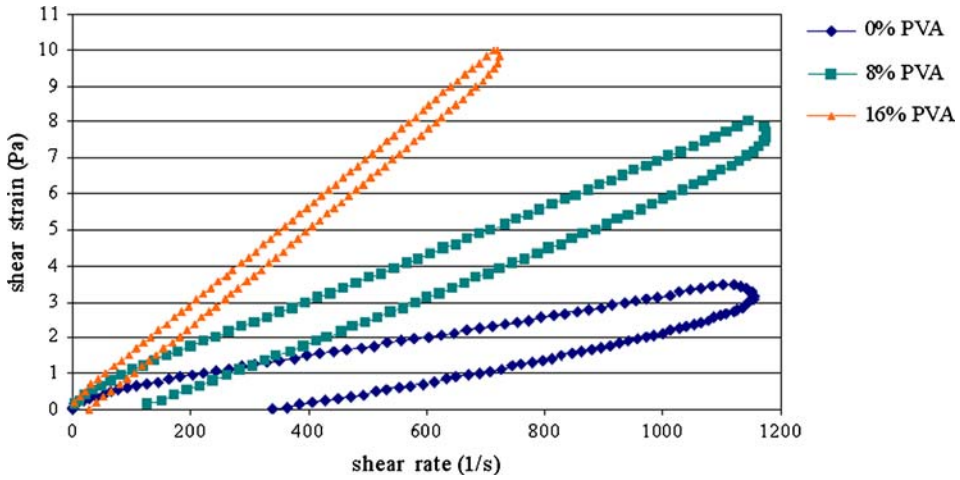

Fig. 4 Shear strain vs. shear rate for three 20 wt.% Y-PSZ aqueous suspensions loaded with 0.17 wt.% PAA and 0, 8, and 16 wt.% PVA, respectively

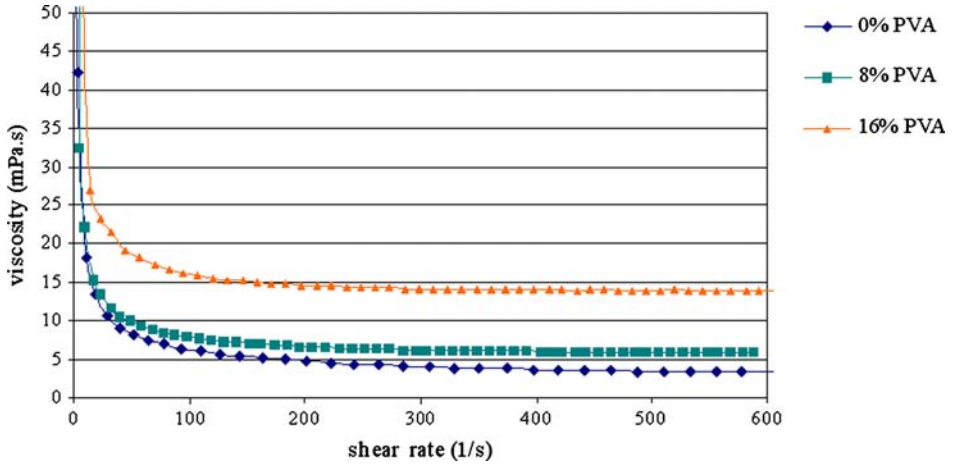

Fig. 5 Evolution of the viscosity vs. shear rate for three 20 wt.% Y-PSZ aqueous suspensions loaded with 0.17 wt.% PAA and 0, 8, and 16 wt.% PVA, respectively

16 wt.% of PVA. All these suspensions were stable and fully dispersed having same surface tension but increasing dynamic viscosity up to 14 mPa.s.

3.2 Characterization of the Suspension Atomization

In co-axial atomization, the shear forces caused by the high-velocity stream of co-flowing gas induce instabilities in the relatively slow-moving liquid jet that force it to break-up. In general, the liquid and gas properties control atomization, especially the droplet size which is a crucial parameter for SPS as it affects the particle momentum. For liquids of low viscosity, the main factors affecting liquid break-up are the surface tension and the aerodynamic forces. Weber dimensionless number, *We*, is used to describe the tendency of the liquid to break-up. *We* is the ratio of the disrupting force related to the dynamic pressure to the consolidating surface tension force: $We = \rho_G V_G^2 d_0/\sigma$ (where ρ_G and V_G are the gas density and gas velocity, respectively, and d_0 a characteristic diameter of the liquid jet). While the Weber number takes into account the forces related to the surface tension, the dimensionless Ohnesorge number, *Oh*, includes the effect of the liquid viscosity. It represents the ratio of the viscous to surface tension forces in the liquid: $Oh = \mu_L/\sqrt{\rho_L \sigma d_0}$ (where μ_L and ρ_L are the liquid dynamic viscosity and density, respectively). The dynamic viscosity, μ_L, causes the liquid to resist the development of instabilities while the surface tension, σ, causes the liquid to resist changes that increases its surface area. The viscosity values used for the calculation of *Oh* numbers are determined at high shear rate (on the flat part of the curves in Fig. 5).

In these experiments, the atomization of the suspension is achieved by a two fluid nozzle in which the energy for atomization is provided by the rapid expansion of argon which is mixed with the suspension within the body of the nozzle. The spray characteristics of such an internal-mixing co-axial twin-fluid atomizer strongly depend on the

interaction between gas and liquid inside the nozzle. In this zone, the major part of the ligament formation and further droplet break-up take place because of the difference in velocity of the two phases and the liquid characteristics related to previously mentioned dimensionless numbers. Various atomization conditions and suspension formulations were combined to change *We* and *Oh* numbers as well as the gas-to-liquid mass flow rate ratio (ALR) values and to assess their influence on the droplets size distribution and spray pattern (Table 2).

For low Weber number (We_G around 5) that means for low gas velocity (V_G of 15 m/s) the droplets size distributions, as determined by light diffusion, are narrow, unimodal, and centered around 300 μm whatever be the Ohnesorge number values (*Oh* of 0.025, 0.038, or 0.083) and hence the liquid characteristics (Fig. 6). This behavior indicates that, in these conditions, the relative velocity is too low to be able to disintegrate the liquid jet into fine droplets even at the lowest dynamic viscosity studied (μ_L of 4 mPa.s). The droplet size distribution is almost unchanged; however, these similar droplets size distributions do not lead to similar spray patterns. It was noticed that when ALR decreases from 0.6 to 0.15 for the low-viscosity suspension formulation the spray shape shrinks (Fig. 7). It could thus be assumed a relation between the ALR value and the spray pattern.

Table 2 *We* and *Oh* numbers and ALR values calculated for various atomization conditions (suspension feed rate and atomizing gas flow rate) and suspension formulations

Suspension	*Oh*	*We*	ALR
Low viscosity (4 mPa.s)	0.025	6	0.6/0.3/0.15
		13	0.3
		24	1.2/0.6/0.3
Medium viscosity (6 mPa.s)	0.038	6	0.6/0.3
		24	1.2/0.6
High viscosity (14 mPa.s)	0.083	6	0.5
		24	1

The increase in the Weber number from 5 to 13 and to 24, while the Ohnesorge number and ALR remain constant (0.025 and 0.295, respectively, corresponding to a low-viscosity suspension), leads to a widening of the droplets size distribution toward finer diameters (Fig. 8). Indeed, three more peaks appear at 12 μm, 30-40 μm and 100 μm which denote a more efficient break-up of the liquid jet as the relative velocity increases from 14 to 21 and to 28 m/s. Simultaneously it was observed that the spray patterns are almost identical (a slight shrinkage is still noticed for the highest suspension feed rate) while the ALR value is constant.

Finally, for ''high'' Weber number, around 24, when Ohnesorge number increases from 0.025 to 0.038 and to 0.083, the droplets size distribution changes from a multimodal to an almost monomodal curve (Fig. 9) as previously described. For such a high *We* value, related to high relative velocities of about 30 m/s, the influence of the suspension characteristics and especially the dynamic viscosity is evidenced. Increasing the *Oh* number causes the suspension to resist the development of instabilities, thus leading to larger droplets sizes. However, the curve related to high *We* and *Oh* numbers still exhibit shoulders in the fine diameter zone whereas this is not the case with low *We* number. Accordingly, the spray pattern shrinks as the ALR value decreases from 1.2 to 0.6 and to 0.3 for high *We* number and low *Oh* number.

3.3 Study of Collected In-Flight Particles and Sprayed Coatings

Owing to the results of the atomization process, three conditions (*We* 6 and *Oh* 0.02 or *We* 24 and *Oh* 0.02 or *We* 24 and *Oh* 0.08) have been selected and injected in a plasma flow according to the operating conditions reported in Table 1. Powders collected in-flight in a water tank have been analyzed in terms of particle size distribution by light scattering after being dispersed in order to avoid agglomeration. For all the powder size distribution curves a peak at 1.4 μm is evidenced whereas in one case a peak at 28 μm is also present (for the high-viscosity

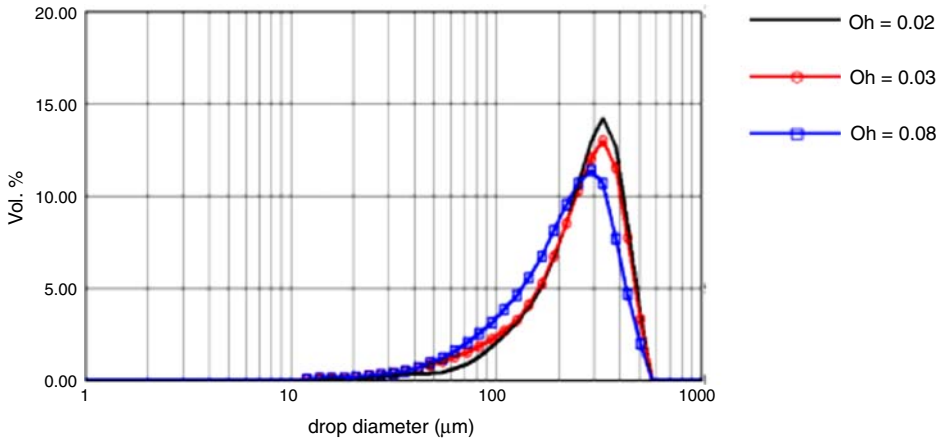

Fig. 6 Comparison of the droplet size distributions for a constant low *We* number (around 6) and several *Oh* numbers

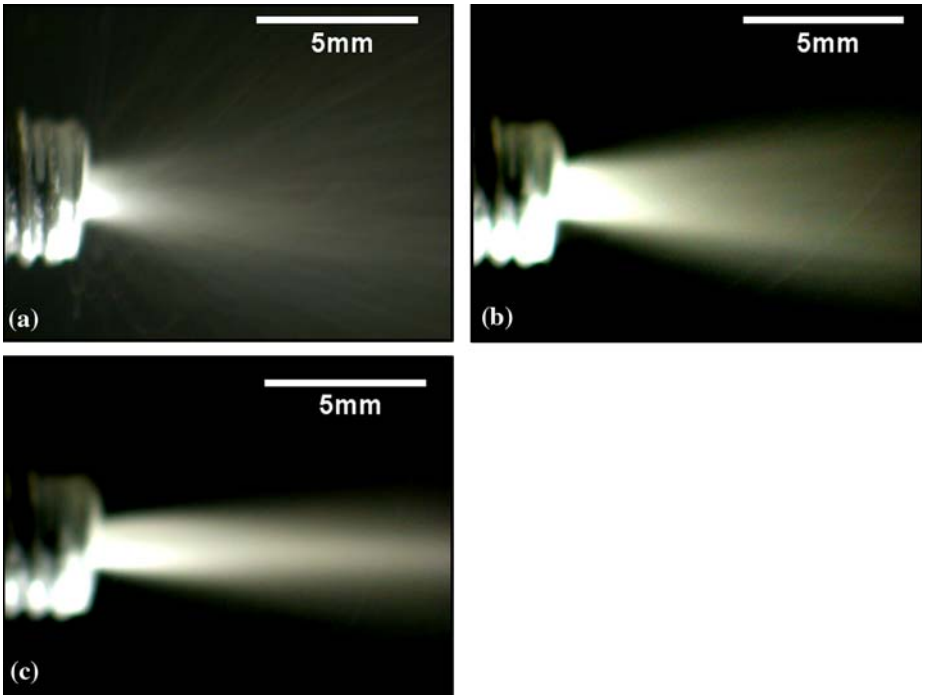

Fig. 7 Spray patterns photographs of low-viscosity Y-PSZ suspensions ($Oh = 0.025$ and $We = 6$) for different ALR values: (a) 0.6, (b) 0.3, and (c) 0.15

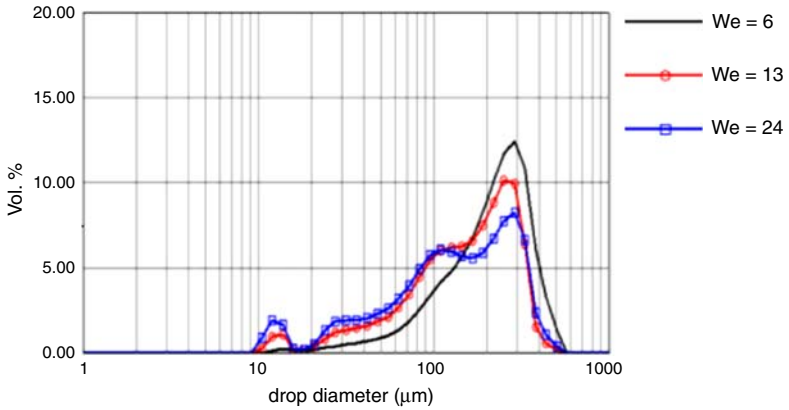

Fig. 8 Comparison of the droplet size distributions for a constant low *Oh* number (0.02) and several *We* numbers

suspension) and in the two other cases (for the low-viscosity suspensions) a peak at 7 μm is shown (Fig. 10). The average droplet sizes from which these three powder sizes originated have been calculated to be, respectively, around 5, 80, and 20 μm (with $\rho_{drop} = 1125$ kg/m^3, $\rho_{YPSZ} = 5860$ kg/m^3, and solid loading of 20 wt.%). The droplet size distributions compared to the powder size distributions and previous calculation make it possible to identify a secondary break-up of the droplets after their injection in the plasma jet. This additional fragmentation of the droplets seems to be influenced by the properties of the suspension, in particular its dynamic viscosity related to the Ohnesorge number. Indeed, large droplet size (centered at 300 μm) combined with high Ohnesorge number (0.08 in the present case) lead to higher collected particle average size (28 μm) than large droplet size combined with low Ohnesorge number (0.02) which lead to collected particle average diameter of 7 μm. In the secondary break-up process, like in the primary atomization, the viscosity of the liquid drop makes it resistant to the development of instabilities and fine fragmentation that would provide with the finer powder size. It has also been noticed that the fraction of fine collected particles (average size around 1.4 μm) seems to correlate with the fraction of fine droplets identified in the sprays.

Coatings have then been manufactured from these three selected sprays and another one based on a *We* number of 6 and an *Oh* number of 0.08 using the same

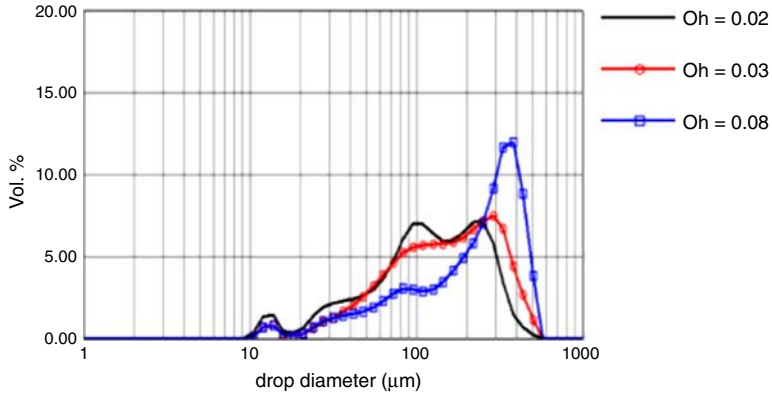

Fig. 9 Comparison of the droplet size distributions for a constant high *We* number (around 24) and several *Oh* numbers

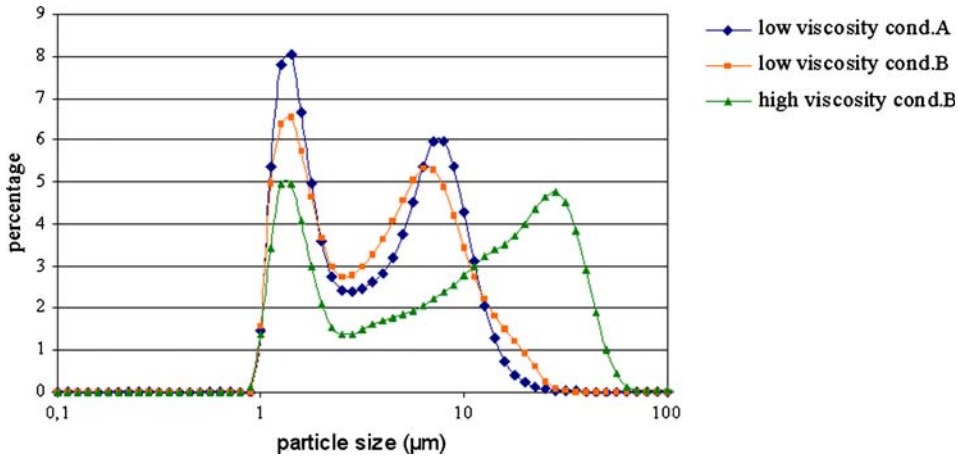

Fig. 10 Comparison of the size distributions of collected particles produced from three sprays: *We* = 6 and *Oh* = 0.02 (low viscosity, condition A) or *We* = 24 and *Oh* = 0.02 (low viscosity, condition B) or *We* = 24 and *Oh* = 0.08 (high viscosity, condition. B)

plasma spray operating conditions (Fig. 11). The deposition efficiency of a coating (Fig. 11) is 2.5 times lower than the one measured for the other coatings (i.e., average thickness equal to 4 µm to be compared to 10 µm). It can be assumed, in this case, that the droplet injection velocity and thus the droplet momentum density is not high enough (related to wide spray pattern as shown in Fig. 7) to permit the major part of the spray to enter the plasma jet and thus allow an efficient injection. The two coatings produced with the same droplet size distribution (*We* 6 and *Oh* 0.02 or 0.08, see Fig. 6) show similar morphological characteristics, in particular a higher density. In contrast, the two coatings originating from the large drop size distribution (i.e., with a noticeable volume fraction of fine droplets during fragmentation, see Fig. 9) exhibit inhomogeneous morphologies with noncohesive, rather powdery, zones. These coatings have been manufactured with suspension atomizing conditions of high ALR, which is related to a high atomizing gas flow rate. Introducing a high-cold atomizing gas flow rate into the plasma flow probably decreases its gas temperature which in turn reduces the heat transferred to the suspension droplets. Such conditions could be detrimental for the coating homogeneity and account for the noncohesive zones. In contrast, the coating morphology seems to be identical whatever the size of the drops originating from the secondary break-up be. This result suggests that the drop trajectories in the plasma allow them to gain enough heat and velocity to impact and adhere on the substrate.

4. Conclusion

The suspension atomization and resulting droplet injection used in the suspension plasma spray process to produce zirconia layers were evaluated versus some suspension characteristics and the atomizer design.

Well-dispersed and stabilized aqueous suspensions have been prepared by adjusting the amount of PAA used as dispersant. A PVA was added to this formulation to adjust the viscosity of the suspension from 4 to 14 mPa.s while the surface tension remained constant at 38 mN/m. The combined effect of the PAA and PVA further

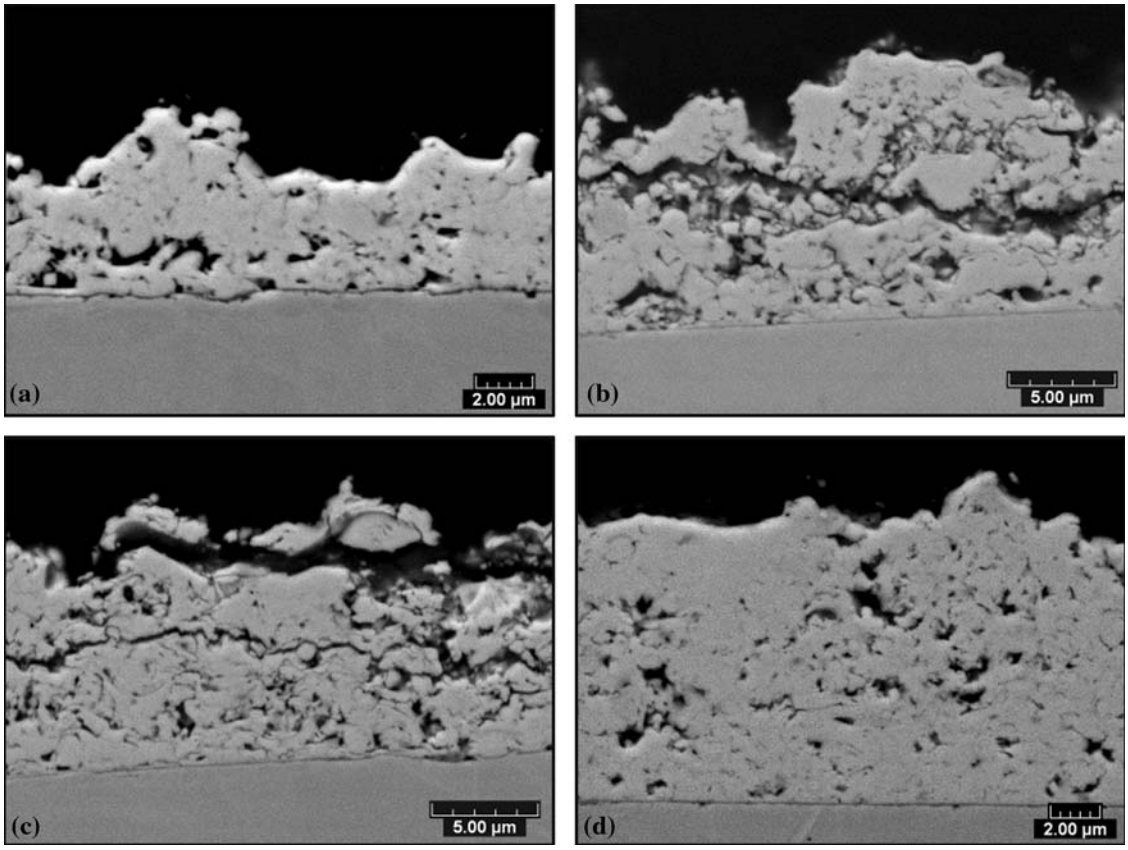

Fig. 11 Cross section views of Y-PSZ coatings produced by SPS of aqueous suspensions: (a) *We* = 6 and *Oh* = 0.02, (b) *We* = 24 and *Oh* = 0.02, (c) *We* = 24 and *Oh* = 0.08, and (d) *We* = 6 and *Oh* = 0.08

improves the dispersion and stability of the suspension probably because of the synergy between the effects of both molecules.

The droplets produced by internal-mixing co-axial twin-fluid atomizer were characterized in size according to two dimensionless numbers (Weber and Ohnesorge numbers) related to surface tension and dynamic pressure or viscosity, respectively. Droplet size distributions were changed from monomodal ones at low *We* to multimodal ones when *We* number increases. At high *We* number, the *Oh* number controls the shape of the droplet size distribution. The relative velocity (of the atomizing gas and liquid jet) and viscosity of the suspensions have a clear influence on the drop size distribution. Moreover, a relation has also been assumed between the spray pattern and the the ALR (gas-to-liquid mass ratio) value. The secondary fragmentation of the droplets due to the plasma jet shear effects was evidenced and the final size of the drops was shown to depend on the characteristics of the suspension, especially the *Oh* number (and thus the viscosity).

Coatings have been sprayed with different deposition efficiencies, which seem to depend upon the velocity of the spray. High atomizing gas flow rate seems to be detrimental to the coating homogeneity. But whatever be the conditions, using aqueous suspension seems to be a promising way to spray rather dense zirconia coatings.

Acknowledgments

This research was financially supported by ANR (National Research Agency) Grant No. 04F364-APURoute ''Characterization of an APU SOFC system for road transport applications''. Authors would like to gratefully acknowledge Dr. P. Bertrand for many fruitful discussions.

References

1. A.R. Nicoll, A. Salito, and K. Honegger, Potential of Plasma Spraying for the Deposition of Coatings on SOFC Components, *Solid State Ionics*, 1992, **52**(1-3), p 269-275
2. T. Yoshida, The Future of Thermal Plasma Processing for Coating, *Pure Appl. Chem.*, 1994, **66**(6), p 1223-1230
3. A. Notomi and N. Hisatome, Application of Plasma Spraying to Solid Oxide Fuel Cell Production, *Pure Appl. Chem.*, 1996, **68**(5), p 1101-1106
4. R. Henne, G. Schiller, V. Borck, M. Mueller, M. Lang, and R. Ruckdaschel, SOFC Components Production—An Interesting Challenge for DC- and RF-Plasma Spraying, *Proceedings of the 15th International Thermal Spray Conference: Thermal Spray Meeting the Challenges of the 21st Century*, C. Coddet, Ed., ASM International, Materials Park, OH, USA, 1998, p 933-938
5. H.C. Chen, J. Heberlein, and T. Yoshida, Preparation of Films for Solid Oxide Fuel Cells by Center-Injection Low Pressure Plasma Spraying, *Proceedings of the 15th International Thermal Spray Conference: Thermal Spray Meeting the Challenges of the 21st Century*, C. Coddet, Ed., ASM International, Materials Park, OH, USA, 1998, p 1309-1314

6. F. Gitzhofer, M. Boulos, J. Heberlein, R. Henne, T. Ishigaki, and T. Yoshida, Integrated Fabrication Processes for Solid-Oxide Fuel Cells Using Thermal Plasma Spray Technology, *MRS Bull.*, 2000, **25**(7), p 38-42
7. J. Will, A. Mitterdorfer, C. Kleinlogel, D. Perednis, and L.J. Gauckler, Fabrication of Thin Electrolytes for Second-Generation Solid Oxide Fuel Cells, *Solid State Ionics*, 2000, **131**, p 79-96
8. O. Yamamoto, Solid Oxide Fuel Cells: Fundamental Aspects and Prospects, *Electrochim. Acta*, 2000, **45**, p 2423-2435
9. A. Weber and E. Ivers-Tiffée, Materials and Concepts for Solid Oxide Fuel Cells (SOFCs) in Stationary and Mobile Applications, *J. Power Sources*, 2004, **127**, p 273-283
10. L.R. Pederson, P. Singh, and X.-D. Zhou, Application of Vacuum Deposition Methods to Solid Oxide Fuel Cells, *Vacuum*, 2006, **80**, p 1066-1083
11. G. Schiller, R.H. Henne, M. Lang, R. Ruckdäschel, and S. Schaper, Development of Vacuum Plasma Sprayed Thin-Film SOFC for Reduced Operating Temperature, *Fuel Cells Bull.*, 2000, **3**(21), p 7-12
12. M. Lang, R. Henne, S. Schaper, and G. Schiller, Development and Characterization of Vacuum Plasma Sprayed Thin Film Solid Oxide Fuel Cells, *J. Therm. Spray Tech.*, 2001, **10**(4), p 618-625
13. M. Lang, R. Henne, S.E. Pohl, G. Schiller, and E. Hubig, Vacuum Plasma Spraying of Thin-Film Planar Solid Oxide Fuel Cells (SOFC)—Development and Investigation of the YSZ Electrolyte Layer, *Proceedings of the International Thermal Spray Conference*, E. Lugscheider, Ed., Verlag, Dusseldorf, Germany, 2002, p 807-812
14. X.Q. Ma, F. Borit, V. Guipont, and M. Jeandin, Vacuum Plasma Sprayed YSZ Electrolyte for Solid Oxide Fuel Cell Application, *Proceedings of the International Thermal Spray Conference*, E. Lugscheider, Ed., Verlag, Dusseldorf, Germany, 2002, p 116-121
15. J. Van Herle, A.J. McEvoy, and K.R. Thampi, Conductivity Measurements of Various Yttria-Stabilized Samples, *J. Mater. Sci.*, 1994, **29**, p 3691-3701
16. K. Okumura, Y. Aihara, S. Ito, and S. Kawasaki, Development of Thermal Spraying-Sintering Technology for Solid Oxide Fuel Cells, *J. Therm. Spray Tech.*, 2000, **9**(3), p 354-359
17. K.A. Khor, L.-G. Yu, S.H. Chan, and X.J. Chen, Densification of Plasma Sprayed YSZ Electrolytes by Spark Plasma Sintering (SPS), *J. Eur. Ceram. Soc.*, 2003, **23**, p 1855-1863
18. K.A. Khor, X.J. Chen, S.H. Chan, and L.-G. Yu, Microstructure-Property Modifications in Plasma Sprayed 20 wt.% Yttria Stabilized Zirconia Electrolyte by Spark Plasma Sintering (SPS) Technique, *Mater. Sci. Eng. A*, 2004, **366**, p 120-126
19. D. Stöver, D. Hathiramani, R. Vassen, and R.J. Damani, Plasma-Sprayed Components for SOFC Applications, *Surf. Coat. Technol.*, 2006, **201**, p 2002-2005
20. J. Karthikeyan, C.C. Berndt, J. Tikkanen, J.Y. Wang, A.H. King, and H. Herman, Preparation of Nanophase Materials by Thermal Spray Processing of Liquid Precursors, *NanoStruct. Mater.*, 1997, **9**, p 137-140
21. J. Karthikeyan, C.C. Berndt, J. Tikkanen, S. Reddy, and H. Herman, Plasma Spray Synthesis of Nanomaterial Powders and Deposits, *Mater. Sci. Eng. A*, 1997, **238**, p 275-286
22. J. Karthikeyan, C.C. Berndt, S. Reddy, J.Y. Wang, A.H. King, and H. Herman, Nanomaterial Deposits Formed by DC Plasma Spraying of Liquid Feedstocks, *J. Am. Ceram. Soc.*, 1998, **81**(1), p 121-128
23. N.P. Padture, K.W. Schlichting, T. Bhatia, A. Ozturk, B. Cetegen, E.H. Jordan, M. Gell, S. Jiang, T.D. Xiao, P.R. Strutt, E. Garcia, P. Miranzo, and M.I. Osendi, Towards Durable Thermal Barrier Coatings with Novel Microstructures Deposited by Solution-Precursor Plasma Spray, *Acta Mater.*, 2001, **49**, p 2251-2257
24. L. Xie, X. Ma, E.H. Jordan, N.P. Padture, D.T. Xiao, and M. Gell, Identification of Coating Deposition Mechanisms in the Solution-Precursor Plasma-Spray Process Using Model Spray Experiments, *Mater. Sci. Eng. A*, 2003, **362**, p 204-212
25. L. Xie, X. Ma, A. Ozturk, E.H. Jordan, N.P. Padture, B.M. Cetegen, D.T. Xiao, and M. Gell, Processing Parameter Effects on Solution Precursor Plasma Spray Process Spray Patterns, *Surf. Coat. Technol.*, 2004, **183**, p 51-61
26. X.Z. Guo, B.G. Ravi, P.S. Devi, J.C. Hanson, J. Margolies, R.J. Gambino, J.B. Parise, and S. Sampath, Synthesis of YTTRIUM GARNET (YIG) by Citrate-Nitrate Gel Combustion and Precursor Plasma Spray Processes, *J. Magn. Magn. Mater.*, 2005, **295**, p 145-154
27. F. Gitzhofer, E. Bouyer, and M.I. Boulos, Suspension Plasma Spray Deposition, U.S. Patent 5 609 921, Mar. 11, 1997
28. M. Bonneau, F. Gitzhofer, and M. Boulos, SOFC/CeO_2 Doped Electrolyte Deposition, Using Suspension Plasma Spraying, *Proceedings of the International Thermal Spray Conference Thermal Spray 2000: Surface Engineering via Applied Research*, C.C. Berndt, Ed., ASM International, Materials Park, OH, USA, 2000, p 929-934
29. P. Fauchais, M. Vardelle, J.F. Coudert, A. Vardelle, C. Delbos, and J. Fazilleau, Thermal Plasma Deposition from Thick to Thin Coatings and from Micro- to Nanostructure, *Pure Appl. Chem.*, 2005, **77**(2), p 475-485
30. P. Fauchais, V. Rat, C. Delbos, J.F. Coudert, T. Chartier, and L. Bianchi, Understanding of Suspension DC Plasma Spraying of Finely Structured Coatings for SOFC, *IEEE Trans. Plasma Sci.*, 2005, **33**(2), p 920-930
31. P. Blazdell and S. Kuroda, Plasma Spraying of Submicron Ceramic Suspensions Using a Continuous Ink Jet Printer, *Surf. Coat. Technol.*, 2000, **123**, p 239-246
32. R. Siegert, J.-E. Döring, J.-L. Marqués, R. Vaßen, D. Sebold, and D. Stöver, Denser Ceramic Coatings Obtained by the Optimization of the Suspension Plasma Spraying Technique, *Proceedings of the International Thermal Spray Conference 2004: Thermal Spray Solutions Advances in Technology and Applications*, ASM International, Materials Park, OH, USA, 2004, p 568-573
33. J. Oberste Berghaus, S. Bouaricha, J.G. Legoux, and C. Moreau, Injection Conditions and In-Flight Particle States in Suspension Plasma Spraying of Alumina and Zirconia Nano-Ceramics, *Proceedings of the International Thermal Spray Conference 2005: Thermal Spray connects: Explore its surfacing potential!*, E. Lugscheider, Ed., Verlag, Dusseldorf, Germany, 2005
34. X.Q. Ma, J. Roth, T.D. Xiao, and M.Gell, Study of Unique Microstructure in SPS Ceramic NanoCoating, *Proceedings of the International Thermal Spray Conference 2003: Advancing the Science and Applying the Technology*, C. Moreau and B. Marple, Eds., ASM International, Materials Park, OH, USA, 2003, p 1471-1476
35. C. Delbos, J. Fazilleau, J.F. Coudert, P. Fauchais, L. Bianchi, and K. Wittman-Teneze, Plasma Spray Elaboration of Finely Structured YSZ Thin Coating by Liquid Suspension Injection, *Proceedings of the International Thermal Spray Conference 2003: Advancing the Science and Applying the Technology*, C. Moreau and B. Marple, Eds., ASM International, Materials Park, OH, USA, 2003, p 661-669
36. C. Delbos, V. Rat, J.F. Coudert, P. Fauchais, and L. Bianchi, Finely Structured Ceramic Coatings Elaborated by Liquid Suspension Injection in a dc Plasma Jet, *Proceedings of the International Thermal Spray Conference 2004: Thermal Spray Solutions Advances in Technology and Applications*, ASM International, Materials Park, OH, USA, 2004
37. J. Fazilleau, C. Delbos, V. Rat, J.F. Coudert, P. Fauchais, and B. Pateyron, Phenomena Involved in Suspension Plasma Spraying Part 1: Suspension Injection and Behavior, *Plasma Chem. Plasma Process.*, 2006, **26**, p 371-391
38. C. Delbos, J. Fazilleau, V. Rat, J.F. Coudert, P. Fauchais, and B. Pateyron, Phenomena Involved in Suspension Plasma Spraying Part 2: Zirconia Particle Treatment and Coating Formation, *Plasma Chem. Plasma Process.*, 2006, **26**, p 393-414
39. A. Ozturk and B.M. Cetegen, Modeling of Axially and Transversely Injected Precursor Droplets into a Plasma Environment, *Int. J. Heat Mass Tran.*, 2005, **48**, p 4367-4383
40. R. Rampon, F.-L. Toma, G. Bertrand, and C. Coddet, Liquid Plasma Sprayed Coatings of Stabilized Zirconia for SOFC Electrolytes, *J. Therm. Spray Tech.*, 2006, **15**(4), p 682-688
41. H. Mahdjoub, P. Roy, C. Filiatre, G. Bertrand, and C. Coddet, The Effect of the Slurry Formulation Upon the Morphology of Spray-Dried Yttria Stabilised Zirconia Particles, *J. Eur. Ceram. Soc.*, 2003, **23**, p 1637-1648